Purdue University
Purdue e-Pubs

International Refrigeration and Air Conditioning
Conference

School of Mechanical Engineering

2012

Comparison of Earth-Air and Earth-Water Ground Tube Heat Exchangers for Residentialal Application

Christophe T'Joen
lliu1@ltu.edu

Liping Liu

M. De Paepe

Follow this and additional works at: http://docs.lib.purdue.edu/iracc

Comparison of Earth-Air and Earth-Water Groud Tube Heat Exchangers for Residential Air-Conditioning Application

C. T'JOEN[1]*, L. LIU[2] and M. De PAEPE[3]

[1] Ghent University – Ugent
Sint-Pietersnieuwstraat 41, 9000, Belgium
christophe.tjoen@ugent.be

[2] Lawrence Technological University,
21000 West Ten Mile Road, Southfield, MI, 48075, USA
lliu1@ltu.edu

[3] Ghent University – Ugent
Sint-Pietersnieuwstraat 41, 9000, Belgium
michel.depaepe@ugent.be

* Corresponding Author

ABSTRACT

Earth-air systems are already commonly applied as a passive technique to reduce the overall energy use of buildings by reducing the required cooling or heating demand. However, they often require large surface area for their installation, and make use of large diameter tubes to reduce the pressure drop. As an alternative, water-earth systems are being considered. To explore these two options, one dimensional analytical models were derived. The impact of different design parameters, including tube length, tube diameter, fluid flow rate, etc., have been investigated. For the earth-air system, it is shown that for high Reynolds numbers, the soil resistance is in fact dominating, and as such this should be carefully considered in the design. For the water-earth systems, the addition of a compact heat exchanger to transfer the heat to the air, has a strong impact on the overall performance compared to an earth-air system. To allow for comparable performance, a compact heat exchanger with a high effectiveness is required (0.8 or higher). A strong interaction between the effectiveness of these two heat exchangers was found as the water flow rate varies. For the earth-water heat exchanger, the soil resistance is even more dominant than for the earth-air system.

1. INTRODUCTION

Rising concerns about the environment (climate change related to CO_2 emissions) and the increasing cost of energy result in an increased number of 'passive' techniques being considered both for new houses and for retrofitting into existing ones. These techniques include improved insulation of roofs and walls, the use of high performance glazing, more efficient heating systems (condensing boilers) and also ground coupled heat exchangers, which are receiving much attention in recent years. These simple heat exchangers are made up of a single tube (or multiple in parallel) through which a fluid is circulated. By placing the tube sufficiently deep (more than 1 m below the surface for a moderate climate zone such as Belgium), the fluid which is circulated can be cooled down in summer and heated up in winter. This is due to temperature lag which occurs between the surface and more profound soil layers. The soil is thus used as a thermal sink and source, providing 'free' heating or cooling, reducing the required heating or cooling capacity to be installed for the house. Next to residential applications, there is a lot of interest from the agricultural sector for usage in the energy intensive greenhouses (Sethi and Sharma, 2008).

Currently most of these systems use ventilation air, and thus make use of large diameter tubes (to reduce the pressure drop). These tubes are made of a polymer to avoid corrosion issues due to the condensing moisture, and

need to be installed carefully to avoid forming stagnant moisture zones (which generate health risks). They also require a considerable length to provide a given capacity (De Paepe and Janssens, 2003), which for a residential application can be difficult to reach due to the plot size. As an alternative, earth-water heat exchangers have been proposed and built. In this case, small diameter tubes are used with water, and an additional heat exchanger (water-air) is then used to transfer heat between the air and water. These systems are thus cheaper and easier to install compared to the air based systems. Some recent applications have been described by Inalli and Esen (2004) and Guo et al. (2012). Congedo et al. (2012) looked at various configurations of water-earth heat exchangers using CFD.

In this paper, one dimensional analytical models are described for an earth-air heat exchanger and an earth-water heat exchanger combined with a compact water-air heat exchanger. These models are used to study the influence of different design parameters (tube length, tube diameter, fluid flow rate, etc.) on the thermal-hydraulic performance.

2. HEAT-EXCHANGER MODELING

2.1 Earth-Air Heat Exchangers (EAHE)
Shown in Fig. 1 is a schematic of earth-air heat exchanger. It is a very simple configuration, a large diameter tube is put into the soil, through which the air flows. The resulting temperature profile is shown in Fig.1 on the right. The soil temperature was set at 10 °C, and air inlet temperature was taken to be 25 °C. Tube material is high-density polyethylene (HDPE) which has a thermal conductivity of 0.2 W/m-K. This is a material commonly used to build these heat exchangers.
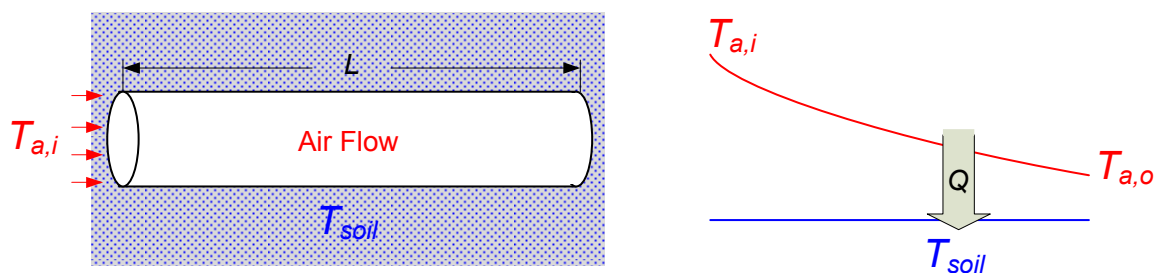

Fig.1 Schematic of an earth-air heat exchanger

If the dimensions of the earth-air heat exchanger are known, computing the heat transfer rate can be done by using either the log-mean-temperature-difference (LMTD) method or the ε-NTU method. In this case, the latter one was used. The air exit temperature was determined from the effectiveness ε, which is a function of the NTU value, as shown in Eqs. (1) - (2). Different NTU relationships exist, which depend on the flow configuration of the heat exchanger (e.g. Kakac and Liu, 2002). For this case, the relationship for an evaporator or condenser (with a constant temperature on one side) was used. The NTU value could be determined from the air flow capacitance C_{air} and the overall conductance, UA, using Eq. (3). The latter was described in Eq. (4) as a sum of the different heat transfer resistances. There are three contributions: conductive resistances through the tube wall and the surrounding soil layer, as well as the convective resistance of the air. Fouling resistance on the air side was neglected. The air-side resistance was determined through Eq. (5) based on known correlations for the Nusselt number. The conductive resistance through the tube wall was determined through Eq. (6). The soil resistance was modelled as a cylindrical layer of soil around the tube with a thickness p, Eq. (7).

$$T_{air,out} = T_{air,in} - \varepsilon \left(T_{air,in} - T_{soil} \right) \tag{1}$$

$$\varepsilon = 1 - e^{-NTU} \tag{2}$$

$$NTU = \frac{UA}{C_{air}} \tag{3}$$

$$\frac{1}{UA} = R_{air} + R_{tube} + R_{soil} \tag{4}$$

$$R_{air} = \frac{1}{h \cdot \pi D_i L} = \frac{1}{Nu \cdot \lambda_a \pi L} \tag{5}$$

$$R_{tube} = \frac{\ln\left(D_o / D_i\right)}{2\pi \lambda_{tube} L} \tag{6}$$

$$R_{soil} = \frac{\ln\left[\left(D_o + 2p\right)/ D_o\right]}{2\pi \lambda_{soil} L} \tag{7}$$

Two correlations were employed for determining the air-side Nusselt number. Equation (8) is valid for laminar flow (Gnielinski, 1983) and Eqs. (9) – (10) are valid for fully turbulent flow (Gnielinski, 1976). The equation for laminar convection is similar to the well known Hausen correlation. Because the Gnielinski correlation for turbulent flow is only valid for Re > 2300, and the laminar correlation predicts a much lower value at Re 2300, an asymptotic blending function (5th order) was used to merge the two correlations (Eq. (11)). This provides a smooth transition between laminar and turbulent flow regimes, as shown in Fig. 2.

$$Nu_{lam} = \left[3.66^3 + 1.61^3 \cdot \left(\frac{Re \cdot Pr \cdot D_i}{L}\right)\right]^{\frac{1}{3}} \tag{8}$$

$$Nu_{turb} = \frac{f_{turb} \cdot \left(Re - 1000\right) \cdot Pr}{2 \cdot \left(1 + 12.7 \cdot \sqrt{\frac{f_{turb}}{2}} \cdot \left(Pr^{\frac{2}{3}} - 1\right)\right)} \tag{9}$$

$$f_{turb} = \left(1.58 \cdot \ln Re - 3.28\right)^{-2} \tag{10}$$

$$Nu = \left(Nu_{lam}^5 + Nu_{turb}^5\right)^{\frac{1}{5}} \tag{11}$$
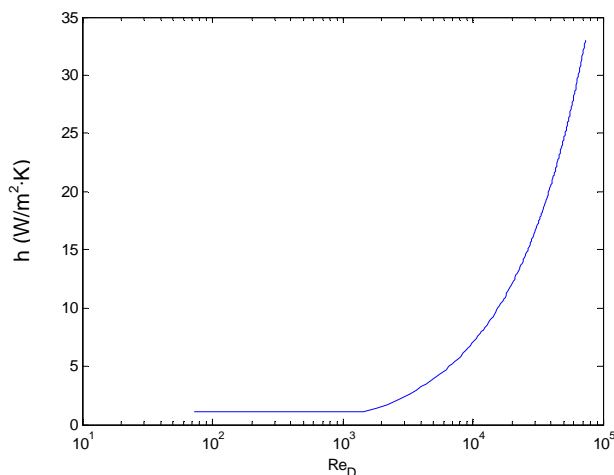

Fig. 2 Air side convective heat transfer coefficient vs. Reynolds number

In terms of the pressure drop performance, a similar approach was adopted, using a 5th order asymptotic blending function between a laminar friction relationship (the Blasius equation, Eq. (12)) and the Filonenko equation (Eq. (10)) which was also used to determine the Nusselt number. All substance properties were evaluated at the average temperature of the fluid stream, therefore the results were obtained in an iterative way. To evaluate the overall thermal-hydraulic performance of a specific configuration, the J-factor, introduced by

De Paepe and Janssens (2003) was used. It is the ratio of the pressure drop to the NTU value, and was shown to be a good performance metric of a ground coupled heat exchanger.

$$f_{lam} = \frac{16}{Re} \tag{12}$$

$$f = \left(f_{lam}^5 + f_{turb}^5\right)^{1/5} \tag{13}$$

$$J = \frac{\Delta P}{NTU} \tag{14}$$

2.2 Earth-Water Heat Exchangers (EWHE)

The earth-water heat exchanger system (Fig. 3) consists of a water loop (indicated in blue) which transfers an amount of heat Q to the soil in the EWHE. The water then absorbs the same amount of heat Q from the air in a compact heat exchanger (CHE). The resulting temperature profiles for both heat exchangers are also shown in Fig. 3. The configuration works in 'cooling mode', and heat is transferred from the air to the soil. However, the reverse option is equally possible, and it results in the same type of equations being used.
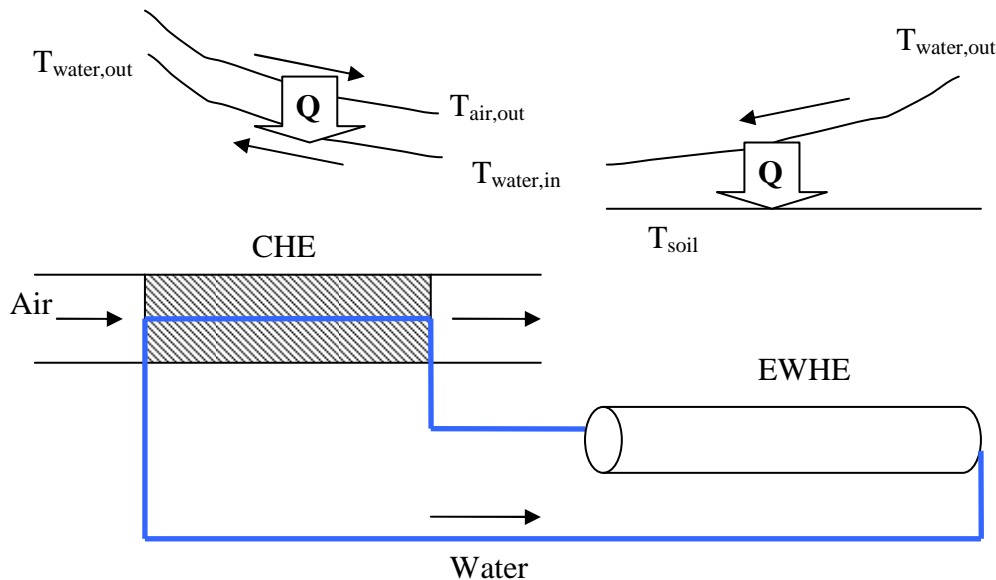

Fig.3 Schematic of an earth-water heat exchanger

Similar to the EAHE, the ε-NTU method was used to model the heat transfer performance. Because there are now two fluid streams, the resulting equations depend on which fluid has the larger capacity rate. By rearranging the different equations for heat transfer in both units, the following equations were derived. The effectiveness of the water-air unit is noted as ε_{WA} and that of the soil-water heat exchanger as ε_{SW}. If $C_{air} < C_{water}$:

$$T_{water,in} = \frac{\varepsilon_{WA} \cdot C_{air} \cdot T_{air,in} - \varepsilon_{WA} \cdot \varepsilon_{SW} \cdot C_{air} \cdot T_{air,in} + \varepsilon_{SW} \cdot C_{water} \cdot T_{soil}}{\varepsilon_{WA} \cdot C_{air} + \varepsilon_{SW} \cdot C_{water} - \varepsilon_{WA} \cdot \varepsilon_{SW} \cdot C_{air}} \tag{15}$$

$$T_{water,out} = \frac{T_{water,in} - \varepsilon_{SW} \cdot T_{soil}}{1 - \varepsilon_{SW}} \tag{16}$$

$$T_{air,out} = T_{air,in} - \varepsilon_{WA} \cdot \left(T_{air,in} - T_{water,in}\right) \tag{17}$$

if $C_{water} < C_{air}$:

$$T_{water,in} = \frac{\varepsilon_{WA} \cdot T_{air,in} - \varepsilon_{WA} \cdot \varepsilon_{SW} \cdot T_{air,in} + \varepsilon_{SW} \cdot T_{soil}}{\varepsilon_{WA} + \varepsilon_{SW} - \varepsilon_{WA} \cdot \varepsilon_{SW}} \tag{18}$$

$$T_{water,out} = \frac{T_{water,in} - \varepsilon_{SW} \cdot T_{soil}}{1 - \varepsilon_{SW}} \qquad (19)$$

$$T_{air,out} = T_{air,in} - \varepsilon_{WA} \cdot \frac{C_{water}}{C_{air}} \left(T_{air,in} - T_{water,in} \right) \qquad (20)$$

Provided the geometries are known for both heat exchangers and the flow rates (allowing computation of the UA values), Eqs. (15) - (20) lead to the determination of the different temperatures shown in Fig. 3. The air inlet temperature and soil temperature were fixed again at 25 °C and 10 °C. Instead of pure water, a mixture of water and ethylene glycol (25% volume) was used with some corrosion inhibitor. The fluid properties of this mixture were modelled through a series of temperature dependant equations. Instead of including all the geometric complexity of the CHE (tube dimensions, fin type, tube layout...), the CHE was modelled simply by a fixed effectiveness ε_{WA}. The same heat transfer and friction correlations as used for the EAHE were used for the WEHE.

3. RESULTS AND DISCUSSION

3.1 Parametric Study on EAHE
A parametric study was conducted based on the conditions in Table 1, under different Reynolds number.

Table 1 EAHE operating conditions

Air inlet temperature	$T_{air,in}$	25 ⁰C
Soil temperature	T_{soil}	10 ⁰C
Soil thermal conductivity	λ_{soil}	1.4 W/mK
Tube wall thickness	t	2.5% of tube inner diameter
Tube thermal conductivity	λ_{tube}	0.2 W/m-K, High-density Polyethylene (HDPE)

Shown in Fig. 4 are the contributions from three thermal resistances as the Reynolds number increases. The left figure shows the absolute values, and the right one relative contribution. During the calculation, the tube length was fixed at 25 m, and 24h penetration depth was taken to be 0.17 m (sandy soil). Three tube diameters were considered (0.11 m, 0.2 m, and 0.4 m), and a constant ratio of tube thickness relative to the tube diameter (2.5%) was employed. This value is based on data from a tube manufacturer. It can be seen from Fig. 4 that with an increasing air speed the impact of the resistance of the tube and the soil increases rapidly. Only at low speeds (Re < 1000) it can be assumed that the air-side resistance is dominant. Also, increasing the diameter results in a decrease in the contribution of soil resistance, given the considered soil volume decreases relative to the considered volume of air. Remarkably, at high velocities the soil resistance dominates. This is an important design consideration. Figure 5 shows the corresponding air outlet temperature of the three tube diameters. As can be seen, for the low Re numbers the effectiveness ~ 1.
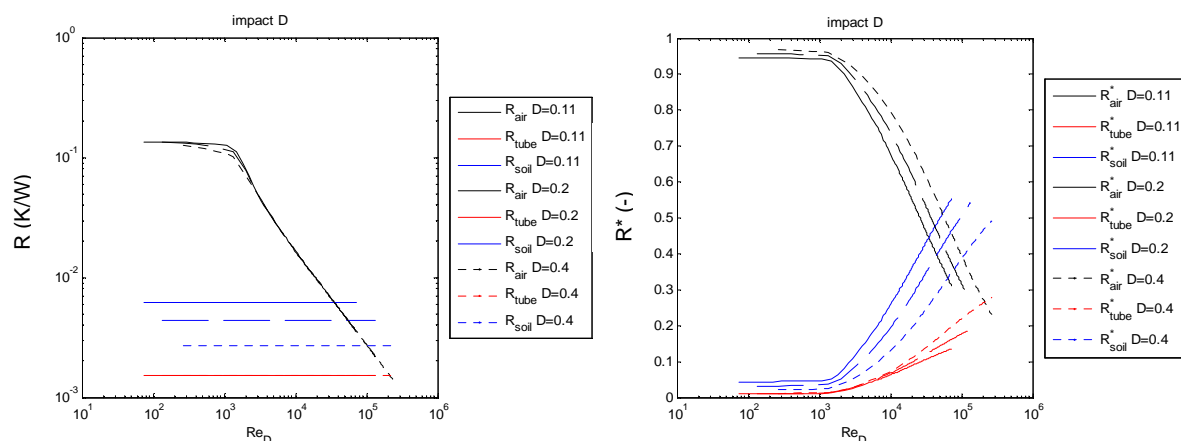

Fig. 4 (L) Various contributions to the heat transfer resistance, constant tube length 25 m, variable air flow and tube diameter; (R) Relative contributions to the resistance to heat transfer, scaled to the total resistance
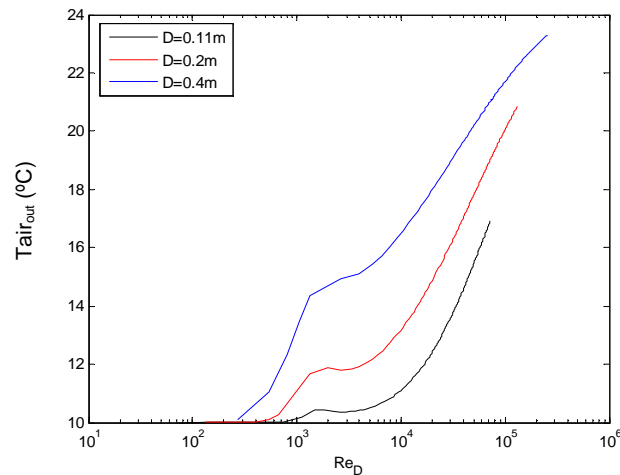
Fig. 5 Outlet temperature of the air-tube heat exchanger, constant tube length 25 m, variable air flow rate and tube diameter

The effectiveness can be used as a design parameter. A typical value to aim for is 0.8, which for an inlet temperature of 25°C corresponds to an outlet temperature of 13°C. Through iteration the tube length required to have $\varepsilon = 0.8$ for different Reynolds numbers can be obtained. The results are shown in Fig. 6. It is clear that using large diameter tubes results in a larger length requirement. In particular for high air flow rates, the required length increases very fast. Around Re ~3000 there is a 'flat' part of the curve, which is caused by the behavior of the Nusselt number in this zone (see Fig. 2).
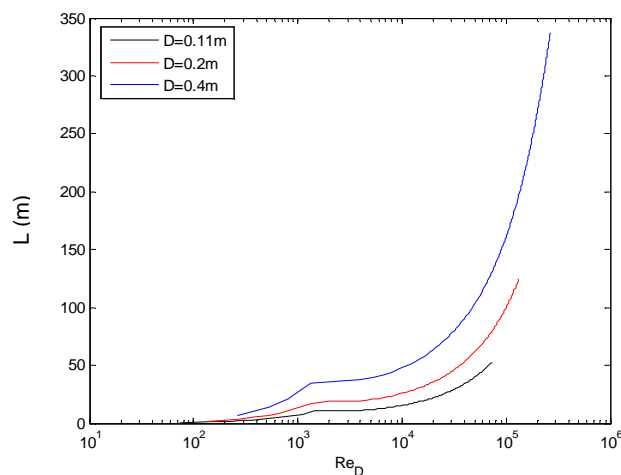

Fig. 6 Required tube length L to reach $\varepsilon = 0.8$ for varying tube diameter and air flow rate.

Different soil types have a different penetration depth, related to their physical properties. For example, clay soils tend to have a smaller penetration depth, about 0.12 m, due to their higher water content. Changing the penetration depth from 0.17 to 0.12 m only shows a small effect. The same was found for the tube wall conductivity. Increasing the tube wall conductivity decreases the conductive heat transfer resistance through the tube wall. However, because R_{tube} only has a small to negligible contribution to the total resistance (see Fig. 3) the effect is very small. The soil conductivity has a stronger impact, which is illustrated in Fig. 7. Note that the selected value of 0.3 W/m-K is an extreme condition, usually soil thermal conductivity varies around 1 - 1.5 W/m-K. Yet it is clear that for high air flow rates, the soil conductivity contributes significantly.
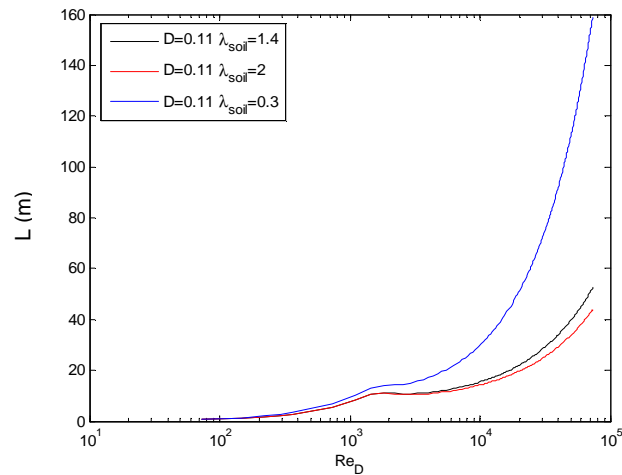
Fig. 7 Required tube length L to reach ε = 0.8 for varying soil thermal conductivity and air flow rate.

3.2 Earth-Water Heat Exchangers (EWHE)

Table 2 EWHE operating conditions

Air inlet temperature	$T_{air,in}$	25 ºC
Soil temperature	T_{soil}	10 ºC
Soil thermal conductivity	λ_{soil}	1.4 W/m-K
Tube wall thickness	t	1.9 mm
Tube thermal conductivity	λ_{tube}	0.2 W/m-K, High-density Polyethylene (HDPE)
Tube diameter	D_i	0.032 m
Water flow rate		500 l/h
Air flow rate		750 m³/h

Because a second heat exchanger is present in this configuration, compared to the EAHE, it is important to assess its impact. Presented in Fig. 8 is the air outlet temperature coming out of the CHE for a varying water tube length and varying CHE effectiveness. The parameters that are fixed are described in Table 2. As shown in Fig. 8, increasing the heat exchanger effectiveness reduces the impact of the CHE, however even at very high effectiveness a large length of tube is needed to reach an 'overall effectiveness' of 0.8 ($T_{air,out}$ = 13°C).
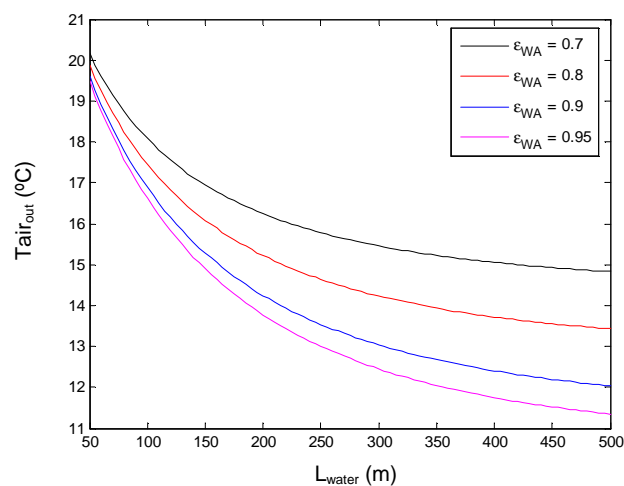

Fig. 8 Air outlet temperature for a varying CHE effectiveness and water side tube length

To explore the potential effectiveness of a CHE, the louvered fin correlation by Wang et al. (1999) was considered. Louvered fin type was used, because it provides the most compact heat transfer solution for air-liquid heat transfer, and it is commonly used for air conditioning applications. Different configurations were

compared, varying the number of screens, the tube diameter, tube spacing, fin spacing, the air channel size and so on. The parameter space was confined to the data listed in the paper by Wang et al. (1999). The results indicated that an effectiveness of 0.8 could be achieved easily and with a good performance (indicated through the J factor for the CHE). The final heat exchanger configuration that was selected has a tube diameter of 6.9 mm, a fin pitch of 2 mm, 6 tube rows, a transversal tube spacing of 25 mm, a longitudinal tube spacing of 21.7 mm and a fin thickness of 0.115 mm. This results in an effectiveness of 0.798. Using a larger channel size on the air side provides a better performance, as it lowers the air velocity, resulting in a significant reduction of the pressure drop. The resulting temperature profiles of the WEHE configuration are shown in Fig. 9. The water tube length is 50 meter, and the CHE geometry described above was used. As can be seen, the air outlet temperature reaches only 15°C. Increasing the water flow rate brings the temperatures closer together. This is due to the interaction between the effectiveness of both heat exchangers: raising the water flow rate increases the effectiveness of the CHE from 0.4 to 0.8 (for the considered Re range), which is due to the decreasing convective water side resistance, but at the same time the effectiveness of the water-soil heat exchanger drops from 0.7 to 0.1, as it has a fixed length of just 50 m. Increasing the tube length further to 150m raises the effectiveness of the water-earth heat exchanger, but the air outlet temperature remains quite high.
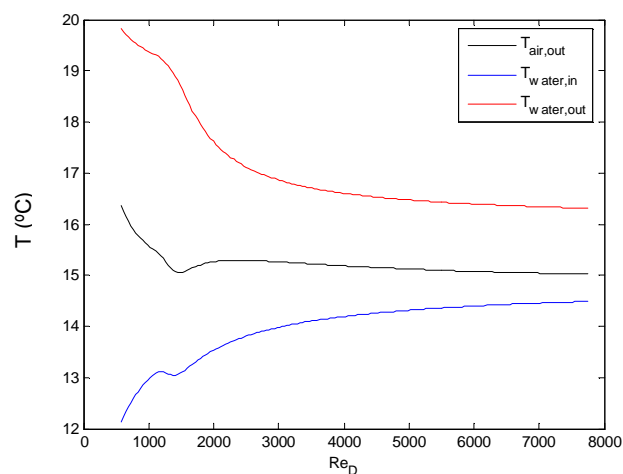
Fig. 9 Temperature profiles for a varying water flow rate for an EWHE

The corresponding contribution of the different thermal resistance components is shown in Fig. 10. It can be seen that increasing the water flow rate has a strong effect initially and as soon as the flow becomes turbulent, the soil resistance becomes dominant. The same soil thickness and properties were considered as in Table 1. As such, for EWHE it is even more important to account for the soil layer in the design than for an EAHE.
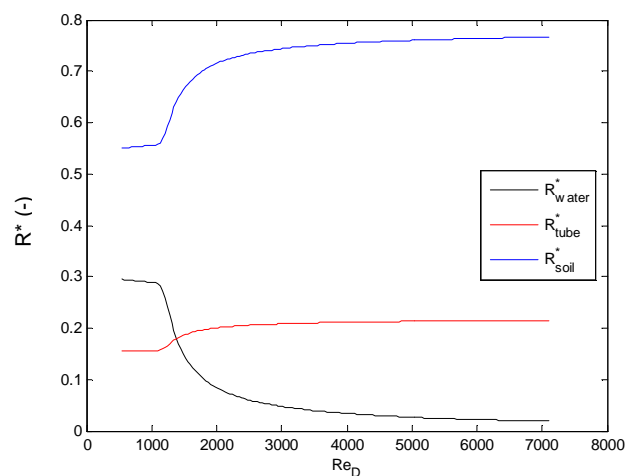
Fig. 10 Relative thermal resistance contribution for a varying water flow rate of an EWHE

3.3 EAHE vs. EWHE

The results above initially seem to indicate that an EAHE can realize a better performance using shorter pipe lengths (though with a significantly larger diameter). As a potential solution to the higher air outlet temperatures, using two CHE in parallel was considered, with the air flowing in series through them. The water flow rate coming from the earth-air heat exchanger is split upstream of the units and then mixed after passing through them. Only a few cases were simulated, but already significant decrease in the outlet temperature was found. For example, when using two of the CHE described above with an air flow rate of 750 m³/h, the outlet temperature drops to 13.7 °C, which is comparable to an EAHE with an effectiveness of 0.8. This makes optimizing the EWHE system more complex and further study should be conducted. An important factor to consider is the final cost of installation. Installing large diameter tubes for a given length requires dedicated ground works, whereas the EWHE system uses small diameter polymer tubes which can be installed much more easily. This should be considered in further studies.

4. CONCLUSIONS

Analytical models were developed for an EAHE and an EWHE combined with a compact water-air heat exchanger. The results show that for both types of heat exchangers, at higher flow rates the thermal resistance of the soil becomes dominant, in particular for the EWHE. This should always be considered in the design process. The CHE effectiveness must be as high as possible. A parameter study of louvered fin units was undertaken to obtain a value of at least 0.8. There is a strong interaction between the two heat exchangers in the EWHE case: when varying the flow rate their effectiveness show an opposite trend. On the whole the required tube installation length is larger for the EWHE compared to an EAHE, but the tubes are much smaller. A few case studies using two CHE in parallel showed further improvement of the EWHE. This should thus be further studied in combination with the economic costs of the total installation.

NOMENCLATURE

C_c	heat capacity rate, W/K			
D	tube diameter, m	*Greek symbols*		
f	friction factor, -	ΔP	Pressure drop, Pa	
h	heat transfer coefficient, W/m^2-K	ε	effectiveness, -	
J	J-factor, ratio of pressure drop to NTU	λ	thermal conductivity, W/m-K	
L	tube length, m			
NTU	number of transfer unit, -			
Nu	Nusselt number, -			
p	penetration depth, m			
Pr	Prandtl number, -	*Subscripts*		
Q	heat transfer rate, W			
R	thermal resistance, K/W	i	inner	
Re	Reynolds number	o	outer	
T	temperature, ⁰C	SW	soil-water	
t	tube wall thickness, m	WA	water-air	
UA	overall thermal conductance, W/K			

REFERENCES

Congedo, P.M., Colangelo, G., and Starace, G., 2012, CFD simulations of horizontal ground heat exchangers: a comparison among different configurations, Applied Thermal Engineering, Vol. 33-34: p. 24-32.

De Paepe, M. De and Janssens, A., 2003, Thermo-hydraulic design of earth-air heat exchangers, Energy and Buildings, Vol. 35: p. 389-397.

Gnielinski, V., 1976, New equations for heat and mass transfer in turbulent pipe and channel flow, International Journal of Chemical Engineering, Vol. 16: p. 359-368.

Gnielinski, V., 1983, Forced convection ducts, in *Heat exchanger design handbook*, Schlünder, Hemisphere, Washington D.C., 2.5.1-2.5.3.

Guo, Y.H., Zhang, G.Q., Zhou, J., Wu, J.S., and Shen, W., 2012, A technoeconomic comparison of direct

expansion ground source and a secondary loop ground coupled heat pump system for cooling in a residential building, Applied Thermal Engineering, Vol. 35: p. 29-39.

Inalli, M. and Esen, H., 2004, Experimental thermal performance evaluation of a horizontal ground-source heat pump system, Applied Thermal Engineering, Vol. 24: p. 2219-2232.

Kakac, S. and Liu, H., 2002, Heat exchangers, selection, rating and thermal design, CRC press.

Sethi, V.P. and Sharma, S.K., 2008, Survey and evaluation of heating technologies for worldwide agricultural greenhouse applications, Solar Energy, Vol. 82: p. 832-859.

Wang, C.C, Lee, C.J., Shang, C.T. and Lin, S.P., 1999, Heat transfer and friction correlation for compact louvered fin-and-tube heat exchangers, International Journal of Heat and Mass Transfer, Vol. 42: p. 1945–1956.